Preliminary Efforts in the Simulation of Molding of a Polypropylene Melt Reinforced with Long Glass Fibers using Transient Shear Rheology

Ortman, K.C.[1], Neeraj Agarwal[1], D.G. Baird[1] and P. Wapperom[2], Jeffrey Giacomin[3]

Chemical Engineering Department[1], Virginia Tech, Blacksburg, VA 24061
Mathematics Department[2], Virginia Tech, Blacksburg, VA 24061
Mechanical Engineering Department[3], University of Madison-Wisconsin, Madison, WI 53706

Abstract

The purpose of this research is to understand the transient fiber orientation and the associated rheology of long glass fiber (> 1mm) reinforced polypropylene, in a well-defined simple shear flow, to extend the results and knowledge gained from these fundamental experiments to the use of simulating (more complex) molding processes. Specifically, we are interested in associating the rheological behavior of glass fiber reinforced polypropylene with the transient evolution of fiber orientation in simple shear flow in an effort to ultimately model fiber orientation in complex flow. A sliding plate rheometer was designed to measure stress growth in the startup and cessation of steady shear flow. Results were confirmed by independent measurements on another sliding plate rheometer[13]. Two fiber orientation models were investigated to predict the transient orientation of the long glass fiber system. One model, the Folgar-Tucker model[2,3] (FT), has been particularly useful for short glass fiber[1] systems and was used in this paper to assess its performance with long glass fibers. A second fiber orientation model[8], one that accounts for the flexibility of long fibers as opposed to rigid rod models commonly used for short fibers, was investigated and results were also compared with experimentally measured values of orientation. The accuracy of these models, when used with the stress tensor predictions of Lipscomb[12], was evaluated by comparing the model predictions against experimental stress growth data. Samples consisting of 10% wt. glass fiber in polypropylene with an average fiber length of 4 mm were prepared with random initial orientation and were sheared at different rates. Model predictions showed that fiber flexibility has the effect of retarding transient fiber orientation but provides poor rheological predictions with the chosen stress model. Additionally, it was shown that the predictions of the Folgar-Tucker model are not able to capture the dynamics of neither the orientation evolution nor the stress growth evolution that was measured experimentally.

Experimental Methods

In this research, the transient startup shear rheology of highly concentrated long glass fibers, in a polypropylene melt, was studied in a sliding plate rheometer. Ten weight percent, 12 mm long glass fibers pellets were extruded and re-pelletized to provide homogeneity. Extrusion does cause fiber breakage. The resulting number average fiber length after extrusion was found to be approximately 4 mm. This material was then compression molded to construct samples of known initial orientation that can be rectilinearly sheared (Figure 1). In this research, samples were subjected to a simple shear flow (Equation 1).

$$v_x(y) = \dot{\gamma}\, y \tag{1}$$

The transient shear rheology was measured using a shear stress transducer. Fiber orientation, within this research, was experimentally measured using the method proposed by Leeds[6]. This method refers to optically analyzing metallographically polished (microtomed) sample slices (in a plane of interest) and determining the tangential orientation from the resulting ellipse.

Fiber Orientation Models

Both the Folgar-Tucker[2] model and Bead-Rod model, suggested by Strautins and Latz[7], were used with the stress predicting Libscomb model to fit model parameters that are most consistent with both the measured orientation evolution and the transient rheology. The accuracy of the models will be discussed. The reader is referred to the literature for model explanations.

Folgar-Tucker Model

The Folgar-Tucker model[2], which has seen much use since its introduction in the 1980's, was developed for short glass fibers in the concentrated regime. Here, the term concentrated is used to describe the ability for significant fiber-fiber interactions to occur. The model has been developed to extend Jeffery's model, introduced in the 1920's, by introducing an isotropic rotary diffusion term. This term, called the Folgar-Tucker term, inhibits the steady state alignment of the fibers from being fully oriented (Equation 2).

$$\frac{D\underline{\underline{A}}}{Dt} = \overbrace{\underline{\underline{A}}\cdot\underline{\underline{\kappa}}^{T} + \underline{\underline{\kappa}}\cdot\underline{\underline{A}} - [(\underline{\underline{\kappa}} + \underline{\underline{\kappa}}^{T}) : \underline{\underline{A}}]\underline{\underline{A}}}^{\text{Generalized Jeffery for Fibers}} + \overbrace{2C_I II_D(\underline{\underline{\delta}} - 3\underline{\underline{A}})}^{\text{Folgar-Tucker Term}} \tag{2}$$

Within this model, D/Dt is the material derivative, $\underline{\underline{\kappa}}^{T}$ is the velocity gradient tensor whose i,jth component is defined as $\partial v_j / \partial x_i$, and C_I is the isotropic rotary diffusion term, II_D is the second invariant of the rate of strain tensor ($\underline{\underline{D}}$) defined as $\underline{\underline{D}} = \frac{1}{2}\left(\underline{\underline{\kappa}} + \underline{\underline{\kappa}}^{T}\right)$, and $\underline{\underline{\delta}}$ is the unit tensor. For the simulation of this model, the quadratic closure approximation is used to decouple to the fourth order orientation tensor (Equation 3).

$$\underline{\underline{A}}_4 = \underline{\underline{A}}\,\underline{\underline{A}} \text{ (quadratic closure approx.)} \tag{3}$$

Because our fibers are long, we wish to explore a model that attempts to account for flexibility.

Bead Rod Model

The model being referred to here was published in 2007 by Strautins and Latz[8]. This Bead Rod model (BR) was published as a continuum fiber model for dilute solutions that provides a first approximation to flexibility. This is accomplished by modeling a fiber as two rods connected by a pivot allowing bead (Figure 2). The model constructs two rigid segments with length l_B that are allowed to slightly pivot about the connecting bead, with some restorative spring rigidity k. Both $\vec{p}$ and $\vec{q}$ are unit vectors that represent the orientation of the corresponding fiber segments, with respect to the center bead. This model makes use of two orientation tensors ($\underline{\underline{A}}$ and $\underline{\underline{B}}$) that represent the second moment of the orientation distribution function with respect to the unit vectors, $\vec{p}$ and $\vec{q}$, in the following manner (Equations 4 and 5).

$$\underline{\underline{A}} = \int \vec{p}\,\vec{p}\,\psi(\vec{p},\vec{q})\,d\vec{p}\,d\vec{q} \tag{4}$$

$$\underline{\underline{B}} = \int \vec{p}\,\vec{q}\;\psi(\vec{p},\vec{q})\,d\vec{p}\,d\vec{q} \tag{5}$$

In simple shear flow, the model's equations are reduced significantly due to the non-existence of second order velocity derivatives. Additionally, we can adapt the isotropic rotary diffusion term of Folgar and Tucker in an ad-hoc manner to probe concentrated suspensions in the following model (Equation 6 and 7).

$$\frac{D\underline{\underline{A}}}{Dt} = \underline{\underline{A}}\cdot\underline{\underline{\kappa}}^T + \underline{\underline{\kappa}}\cdot\underline{\underline{A}} - [(\underline{\underline{\kappa}} + \underline{\underline{\kappa}}^T) : \underline{\underline{A}}]\underline{\underline{A}} - 2k[\underline{\underline{B}} - \underline{\underline{A}}\ tr(\underline{\underline{B}})] - 6C_I II_D\left(\underline{\underline{A}} - \frac{1}{3}\underline{\underline{\delta}}\right) \tag{6}$$

$$\frac{D\underline{\underline{B}}}{Dt} = \underline{\underline{B}}\cdot\underline{\underline{\kappa}}^T + \underline{\underline{\kappa}}\cdot\underline{\underline{B}} - [(\underline{\underline{\kappa}} + \underline{\underline{\kappa}}^T) : \underline{\underline{A}}]\underline{\underline{B}} - 2k[\underline{\underline{A}} - \underline{\underline{B}}\ tr(\underline{\underline{B}})] - 6C_I II_D\left(\underline{\underline{B}} - \frac{tr(\underline{\underline{B}})}{3}\underline{\underline{\delta}}\right) \tag{7}$$

The physical interpretation of the $\underline{\underline{A}}$ tensor is that it describes the orientation tensor of a given rod, either $\vec{p}$ or $\vec{q}$. The $\underline{\underline{B}}$ tensor, on the other hand, describes the end-to-end distance between the two rods at any given time and thus, in simple flows where no second order velocity gradients exist, behaves as a time delay for the model fiber to "open" (provided it has some initial bending to it). To take advantage of this time delayed effect, we wish to phenomenologically choose to use an orientation tensor constructed from the dimensionless end-to-end vector (Equation 8), (Figure 3). This choice will give us a little more control over the dynamics of the orientation evolution.

$$\vec{r} = \vec{p} - \vec{q} \tag{8}$$

Using this definition of the end-to-end vector, an analogous definition of the orientation tensor (constructed from the end-to-end vector) can be formed by taking the second moment of this vector with respect to the orientation tensor (Equation 9).

$$\underline{\underline{rr}} = \int \vec{r}\vec{r}\ \psi(\vec{p},\vec{q},t)d\vec{p}\,d\vec{q} \tag{9}$$

This form of the orientation tensor is not fully useful because it has not yet been normalized. Hence, the normalized form of this tensor is obtained by dividing the tensor by the magnitude of the end-to-end vector. This is equivalent to normalizing the tensor with respect the trace of this tensor to form (Equation 10).

$$\underline{\underline{R}} = \frac{\underline{\underline{rr}}}{tr(\underline{\underline{rr}})}(\text{normalized end-to-end tensor}) \tag{10}$$

Libscomb Stress Model

The Libscomb stress model was used in this research to relate the transient fiber orientation within the melt to the transient viscosity behavior of the suspension. The quadratic closure approximation was again used. The orientation representation that we have chosen to use in this model was of the end-to-end form (Equation 10). With this adaptation, the Libscomb model[12] for the transient shear viscosity (η^+) becomes (Equation 11).

$$\eta^+ = \eta_s + c_1\varphi\eta_s + 2\varphi\eta_s N R_{12}^2 \tag{11}$$

In this expression, η_s is the neat matrix viscosity, φ is the volume fraction of fibers, c_I is a coefficient responsible for the viscosity enhancement due to the presence of fibers, N is a parameter associated with the enhancement due to fiber orientation, and R_{12} is the 1-2 component of the orientation tensor. It is worth mentioning, for the case of Folgar-Tucker, that the orientation tensor ($\underline{\underline{A}}$) of a rigid rod is the same as its end-to-end orientation ($\underline{\underline{R}}$) because a rigid rod does not bend. For concentrated suspensions, both c_I and N were used as fit parameters for this stress model.

Results

Extruded long glass fiber strands (with a post-extruded average fiber length of 4 mm) were given an initially random planar orientation and sheared for 70 strain units at shear rates of 0.4, 1.0, and 4.0 sec^{-1}. The transient rheologies of the fiber suspensions are shown in (Figure 4). As one can see, the shear stress overshoot are larger at lower shear rates. Likewise, shear thinning is also visible. These effects have been reported in literature and have been said to be due to long fiber flocculation[14]. At higher shear rates, the aggregates are more easily broken and hence lower peaks and steady state viscosities are realized. The corresponding orientation evolution at 1.0 sec^{-1} is depicted in (Figure 5 and 6).

Using this orientation information, the orientation model parameters can be fit. Initial conditions of the orientation models for planar random fibers are $A_{11}=A_{33}=1/2$, $A_{ij\neq 11,33}=0$, and $B_{ij}=0$. These conditions infer that the end-to-end orientation tensor has the initial conditions of $R_{11}=R_{33}=1/2$, $R_{ij\neq 11,33}=0$. One disadvantage of the Folgar-Tucker model is that the orientation kinetics cannot be slowed down. This is untrue for the relatively new 'Reduced Strain Closure' model of Tucker, et al.[15], but this form will not be evaluated in this paper. Using the original form of the Folgar-Tucker model, the isotropic rotary diffusion coefficient (C_I) may be fit to obtain the largest strain value of the A_{11} component of the orientation tensor given in (Figure 5). Ideally, this value should conform to the steady state value of the transient orientation, but the data at 70 strain units shown in (Figure 5) is the closest value available to the true steady state orientation. This same value will also used in the Bead Rod model, but k may be varied to either slow or speed up the orientation kinetics, in this situation. It is very important to reiterate the distinction between these two models again. The Bead Rod model was used in this paper to slow orientation kinetics by giving the fibers a random in-plane orientation, identical to that used by the Folgar-Tucker model, but also with a random initial bending angle (not found in rigid rod theory such as the Folgar-Tucker model). This allows the restorative spring rigidity k to be varied and behave as a time delayed orientation parameter, as mentioned before. The isotropic rotary diffusion term was found to be $C_I = 0.038$ to asymptotically approach the largest strain value of orientation available. Using a least squared error method, the bending rigidity term of the Bead-Rod model was determined to be $k = 0.012$. Using these parameters, the orientation model predictions can be compared with the experimentally determined values (Figure 7 and 8).

As one can see from (Figures 7 and 8), the Folgar-Tucker model over predicts the rate of orientation. The Bead-Rod model, on the other hand, approaches the predictions of the Folgar-Tucker more slowly. One important difference is apparent in (Figure 8). The models' values of the 1-2 component of the orientation tensor converge in (Figure 8), but the Bead-Rod model shows no overshoot. This is especially apparent when the orientation models are used in combination with the Libscomb model to predict the transient stress growth (Figure 9).

For the 10% wt. glass fiber systems of interest, the volume fraction of fiber is $\varphi=0.038$, and the neat polyproplene matrix viscosity is $\eta_s=560$ Pa*sec at a shear rate of 1.0 sec^{-1}. The stress model

parameters (c_1 and N), in combination with the orientation models and their respective model parameters already determined from the transient orientation data, were also determined by using a minimized error approach. Despite the small viscosity overshoot predicted by using the Folgar-Tucker model (in combination with the stress model), it is not able to capture the magnitude of the overshoot. The Bead Rod model, on the other hand, does not show even a slight overshoot prediction and overall produces a rather trivial and useless viscosity profile. Additionally, when the Bead Rod model, and its parameters that were determined from one set of data, are used to predict the orientation evolution and corresponding rheology at a shear rate of 4.0 sec^{-1}, it produces results that are further incorrect. Specifically, the orientation versus strain profile is predicted to be even slower than what was fit at 1.0 sec^{-1}. This is because the delay in orientation is based on time and not strain, thus effectively retarding the orientation evolution even more drastically. This is incorrect because, although not shown in this paper, experimentally we see fibers align more quickly at higher shear rates. Again, this retardation completely eliminates the prediction of a viscosity overshoot and hence provides a particularly poor understanding of the rheology. It is apparent from this treatment that neither of these orientation models can be used with the stress model chosen to accurately relate the transient rheology with the underlying fiber orientation.

Summary and Conclusion

An orientation model that tries to account for flexibility was used with the stress predicting Libscomb model to try to link the rheological behavior of long glass fiber reinforced polypropylene to its fiber orientation microstructure. Additionally, the much more widely acknowledged Folgar-Tucker model was used as a standard for comparison. Orientation model parameters were fit from transient orientation data, and stress model parameters were fit from simple shear flow rheology, both at a shear rate of 1.0 sec^{-1}. It was shown that the orientation and stress models used in this paper are not fully consistent with experimentally determined values. This is apparent in the lack of ability of either model to accurately capture the dynamics of the measured transient rheology. Notably, the Bead Rod model does not show an overshoot in the A_{12} component with increased flexibility, and thus provides poor rheology predictions with the chosen stress model. Additionally, when the Bead Rod model is used in the manner describe by this paper, it predicts slower orientation kinetics at higher shear rates, which is in contradiction with experiment. The fundamental goal of this research is to accurately predict complex flow processes involving long glass fibers, but a better combination of orientation and stress model may still be needed.

Acknowledgments

Financial of NSF: DMI-0853537

Figure Appendix:

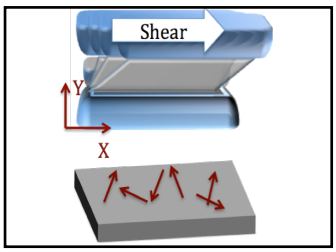

Figure 1: Illustration of a compression molded sample containing planar random initial fiber orientation (below) in a sliding plate apparatus (above).

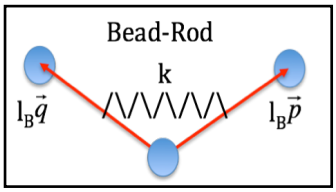

Figure 2: Fiber model, with segment length l_B, allowing semi-flexibility. The segment orientations are denoted by unit vectors $\vec{p}$ and $\vec{q}$, and resist bending by some spring constant k.

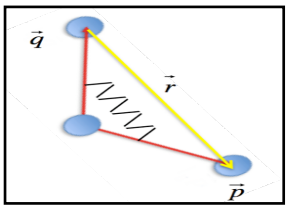

Figure 3: Illustration of the dimensionless end-to-end vector of a bead-rod model fiber.

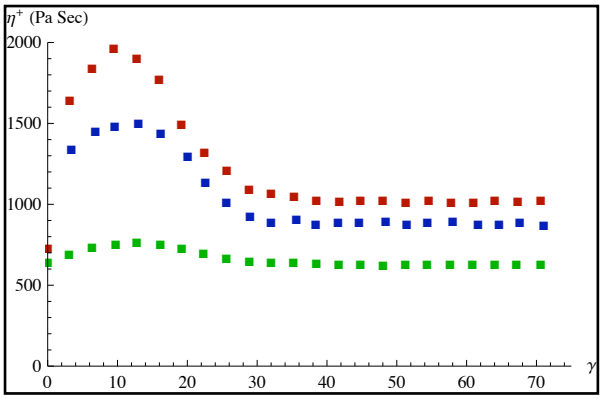

Figure 4: Experimentally measured transient viscosity vs. strain for 10% long glass fibers initially oriented randomly in the shear plane, at various shear rates [■=0.4 sec^{-1}, ■=1.0 sec^{-1}, ■=4.0 sec^{-1}]

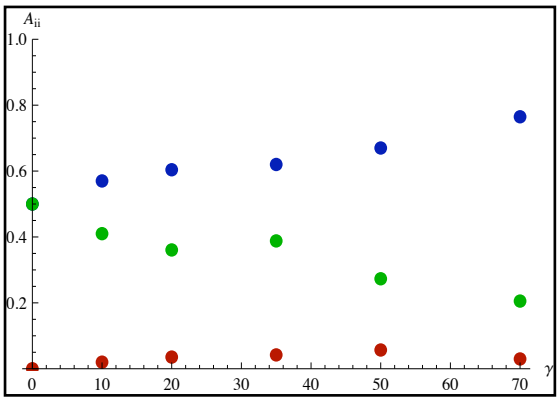

Figure 5: Experimentally determined data for the orientation evolution of the trace components of the orientation tensor versus strain at a shear rate of 1.0 sec^{-1}. System is 10% wt. glass fibers initially random in shear plane. [Data=Points, ●=A_{11}, ●=A_{22}, ●=A_{33}]

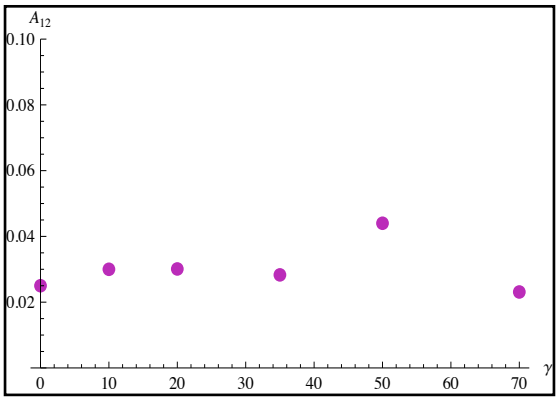

Figure 6: Experimentally determined data for the orientation evolution of the 1-2 component of the orientation tensor versus strain at a shear rate of 1.0 sec^{-1}. System is 10% wt. glass fibers initially random in shear plane. [Data=Points, ●=A_{12}]

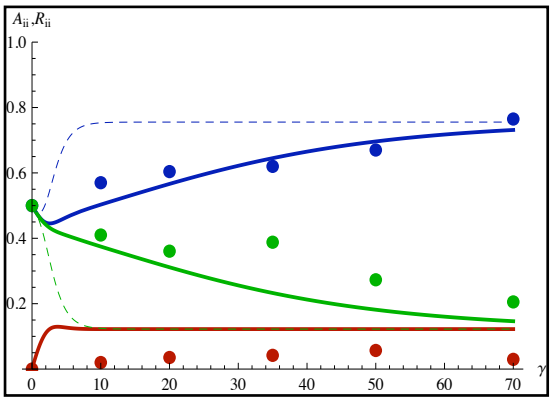

Figure 7: Experimentally determined data and model predictions for the orientation evolution of the trace components of the orientation tensor (A_{ii} for Folgar-Tucker and Data, and R_{ii} for the Bead Rod model) versus strain at a shear rate of 1.0 sec^{-1}. System is 10% wt. glass fibers initially random in shear plane. C_I =0.038, k =0.012. [Data=Points, FT=Dashed, BR=Solid, ●=A_{11},R_{11}, ●=A_{22},R_{22}, ●=A_{33},R_{33}]

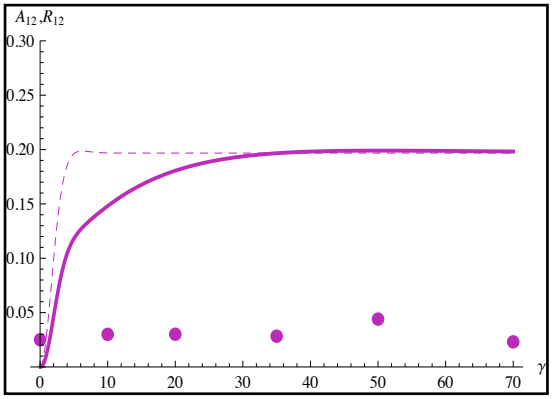

Figure 8: Experimentally determined data and model predictions for the orientation evolution of the 1-2 component of the orientation tensor (A_{12} for Folgar-Tucker and Data, and R_{12} for the Bead Rod model) versus strain at a shear rate of 1.0 sec^{-1}. System is 10% wt. glass fibers initially random in shear plane. C_I =0.038, k =0.012. [Data=Points, FT=Dashed, BR=Solid, ●=A_{12},R_{12}]

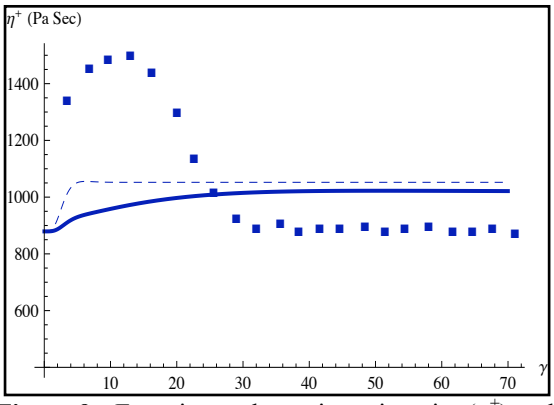

Figure 9: Experimental transient viscosity (η^+) and model fits (using the orientation models in combination with the stress Libscomb model) for fibers initially random in plane and sheared at 1.0 sec^{-1}. [■=1.0 sec^{-1}, Data=Points, FT=Dashed, BR=Solid]. [Model Parameters for FT: C_I=0.038, c1=15, N=105. Model Parameters for BR: C_I=0.038, k=0.012, c_1=15, N=85].

References

1. Eberle, A., et al., *J. Rheol.* **53**, 685-706 (2008).
2. Advani, S.G., and Tucker III, C.L., *J. Rheol*. **31**, 751-84 (1987).
3. Advani S.G. and Tucker III C.L., *J. Rheol*. **34,** 367-386 (1990).
4. Baird D. G. and Collias, D. I., Polymer Processing, Boston: Butterworth-Heinemann, 1998.
5. Folgar, F. P. and Tucker III, C. L., *J. Reinf. Plast. Comp.* **3**, 98-119 (1984).
6. Hine, P.J., Davidson, N., Duckett, R.A., *Poly. Comp.* **17**, 720–729 (1996).
7. Bay R. S. and Tucker III, C. L., *Polym Eng Sci.* **32**, 240-253 (1992).
8. Strautins, U. and Latz,A., *Rheol. Acta.* **46**. 1057-1064 (2007).
9. Smith, W. and Hashemi, J., Foundations of Material Science and Engineeering. *McGraw Hill* (2006)
10. Junke, X. and Costeux, S., *Rheo. Acta.* **46**, 815-824 (2007).
11. Velez-Garcia, G., Ortman K., *ICOR Conf. Proc.* **1027**, 42-44 (2008).
12. Lipscomb, G., et al., *J. Non-Newt. Fluid. Mech*. **26**, 297–325 (1988).
13. Kolitawong, C. and Giacomin, A.J., J. Non-Newt. Fluid. Mech. **102**, 71-96 (2002).
14. Keshtkar, M., et al., J. Rheol., 2009. 53: p. 631-650.
15. Wang, J., O'Gara, J., and Tucker III, C. L., *J. Rheol.* **52**(5), 1179-1200 (2008).

Key Words: Long glass fiber rheology, long glass fiber orientation, sliding plate rheometer, flexible fiber, composite, glass reinforced thermoplastic